JOURNAL OF VIROLOGY, Apr. 2011, p. 3095–3105 Vol. 85, No. 7
0022-538X/11/$12.00 doi:10.1128/JVI.02360-10

Rotavirus VP2 Core Shell Regions Critical for Viral Polymerase Activation▽†

Sarah M. McDonald* and John T. Patton

Laboratory of Infectious Diseases, National Institute of Allergy and Infectious Diseases, National Institutes of Health, Bethesda, Maryland 20892

Received 11 November 2010/Accepted 10 January 2011

The innermost VP2 core shell of the triple-layered, icosahedral rotavirus particle surrounds the viral genome and RNA processing enzymes, including the RNA-dependent RNA polymerase (VP1). In addition to anchoring VP1 within the core, VP2 is also an essential cofactor that triggers the polymerase to initiate double-stranded RNA (dsRNA) synthesis using packaged plus-strand RNA templates. The VP2 requirement effectively couples packaging with genome replication and ensures that VP1 makes dsRNA only within an assembling previrion particle. However, the mechanism by which the rotavirus core shell protein activates the viral polymerase remains very poorly understood. In the current study, we sought to elucidate VP2 regions critical for VP1-mediated *in vitro* dsRNA synthesis. By comparing the functions of proteins from several different rotaviruses, we found that polymerase activation by the core shell protein is specific. Through truncation and chimera mutagenesis, we demonstrate that the VP2 amino terminus, which forms a decameric, internal hub underneath each 5-fold axis, plays an important but nonspecific role in VP1 activation. Our results indicate that the VP2 residues correlating with polymerase activation specificity are located on the inner face of the core shell, distinct from the amino terminus. Based on these findings, we predict that several regions of VP2 engage the polymerase during the concerted processes of rotavirus core assembly and genome replication.

Rotaviruses are enteric pathogens and a leading cause of severe diarrhea in infants and young children (3). Like other segmented, double-stranded RNA (dsRNA) viruses of the family *Reoviridae*, rotaviruses perform all stages of viral RNA synthesis within the confines of proteinaceous particles (15, 16). The infectious virion consists of three concentric protein layers surrounding 11 unique dsRNA genome segments (6, 20). The outermost virion layer is composed of the glycoprotein (VP7) and the spike protein (VP4), while the intermediate layer is made exclusively of VP6 (6, 20). The innermost layer of the rotavirus particle, referred to as the core shell, is a T=1 icosahedron composed of VP2 (9, 10, 12). Complexes containing the RNA-dependent RNA polymerase (VP1) and the capping enzyme (VP3) are located beneath VP2, in proximity of the 5-fold axes (6, 20). The viral dsRNA genome, which codes for six structural and five or six nonstructural proteins, is thought to be organized as tubules that spool around the enzymes and pack tightly against the core shell (3, 12). A VP1 monomer is dedicated to transcribing and replicating an associated genome segment, presumably while tethered to the VP2 interior (5, 15). However, the role of VP2 extends beyond serving as a scaffold for the viral polymerase; it is also a critical cofactor that causes VP1 to initiate genome replication (dsRNA synthesis) (19, 24).

The structural architecture of the rotavirus VP2 core shell has been determined at high resolution using cryo-electron microscopy and X-ray crystallography (9, 10, 12, 27). The results show a relatively smooth icosahedron, ~50 nm in diameter, comprised of 120 copies of VP2 organized into 12 decameric units (Fig. 1) (9, 10, 12, 27). Each decamer is made up of two structurally distinct, but chemically identical, forms of the protein (type A and B VP2) (Fig. 1) (9, 10, 12, 27). Five type A VP2 monomers converge around the 5-fold axis, while five type B monomers sit further back and intercalate between the type A molecules (Fig. 1) (9, 10, 12, 27). The principal domain of rotavirus VP2 (residues ~100 to 880) folds into a thin, comma-shaped plate, which can be structurally delineated into three subdomains (12). The extreme amino-terminal residues of VP2 (residues ~1 to 100 of type A and ~1 to 80 of type B) are not fully resolved in any known structure. However, the X-ray crystallographic data for bovine rotavirus double-layered particles (DLPs) reveal a cylindrical feature underneath each 5-fold axis (12). This internal protrusion, referred to as the 5-fold hub, is attributed to the first ~100 residues of 10 abutting VP2 monomers. The 5-fold hub has been predicted to form a conduit for the exit of nascent plus-strand RNA transcripts following their synthesis by VP1 within transcriptionally active DLPs (12).

Previous biochemical studies indicated that the VP2 5-fold hub is also important for interactions with VP1. Specifically, the deletion of residues 1 to 92 does not affect the capacity of recombinant VP2 to form core-like particles but does abrogate VP1 (and VP3) encapsidation into those assemblies (9, 26). Likewise, VP2 lacking the amino-terminal 27 residues is not capable of supporting efficient VP1-mediated *in vitro* dsRNA synthesis, suggesting that the 5-fold hub plays a role in polymerase activation (19). The molar ratio of VP2 to VP1 for optimal *in vitro* genome replication is 10:1, indicating that a

* Corresponding author. Mailing address: Laboratory of Infectious Diseases, National Institute of Allergy and Infectious Diseases, National Institutes of Health, 50 South Drive, Room 6311, Bethesda, MD 20892-8026. Phone: (301) 594-1663. Fax: (301) 496-8312. E-mail: mcdonaldsa@niaid.nih.gov.

† Supplemental material for this article may be found at http://jvi.asm.org/.

▽ Published ahead of print on 19 January 2011.

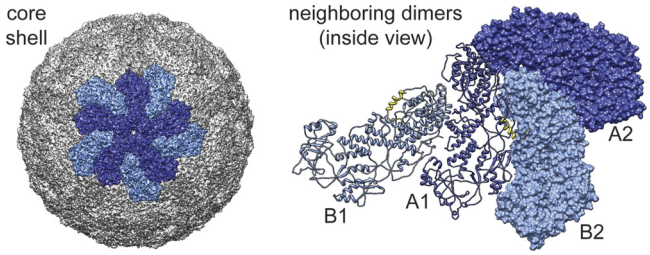

FIG. 1. Structure of the rotavirus VP2 core shell. (Left) Structure of the T=1 icosahedral core shell of bovine rotavirus (PDB accession number 3KZ4), with each of the 120 VP2 monomers depicted in a surface representation. Five type A and five type B VP2 monomers of a central decamer are in dark blue and light blue, respectively. (Right) Inside view of two neighboring VP2 A-B dimers. Type A and B monomers are in dark blue and light blue, respectively. One of the dimers (comprised of monomers A1 and B1) is depicted in a ribbon representation, while the other (comprised of monomers A2 and B2) is depicted in a surface representation. The resolved portion of the VP2 amino terminus in type B monomers (residues 81 to 100) is yellow and is shown in a ribbon representation.

VP2 decamer (or 5-fold hub thereof) triggers a VP1 monomer (19, 24). In addition to VP1 binding, residues of the 5-fold hub have also been implicated in nonspecific interactions with nucleic acid (8). Nonetheless, VP1 is capable of recognizing viral plus-strand RNA in the absence of VP2, indicating that the core shell requirement for enzyme activity is not merely a reflection of template recruitment (11, 17, 24). In a previous study, we showed that VP1 proteins of genetically divergent rotavirus strains (SA11 and Bristol) are capable of mediating *in vitro* dsRNA synthesis using each other's plus-strand RNA templates but that they require their cognate core shell proteins for enzymatic activity (13). This result provides solid evidence that there is a direct and specific interaction between VP1 and VP2 during genome replication. VP2 is essential, along with plus-strand RNA, GTP, and Mg^{2+}, for the creation of a salt-stable VP1 initiation complex, which is a prerequisite for phosphodiester bond formation (24). Based on the available data, it is hypothesized that an assembling VP2 core directly engages VP1 bound to one of 11 unique plus-strand RNA templates. This VP1-VP2 interaction induces structural changes in the polymerase that allow it to initiate dsRNA synthesis and create the viral genome (11, 14, 23). The requirement for VP2 ensures that VP1 makes dsRNA only when inside a particle that is the morphogenic precursor to an infectious virion, thus serving to couple assembly, packaging, and genome replication. Still, the molecular mechanism by which VP2 activates VP1 remains very poorly understood.

In this study, we sought to elucidate rotavirus VP2 core shell regions critical for polymerase activation. Using amino acid sequence and structural predictions, we engineered mutant VP2 proteins and assayed them for the capacity to support VP1-mediated *in vitro* dsRNA synthesis. We found that although the VP2 amino terminus is important for VP1 activation, the residues that correlate with polymerase specificity are located on the inner face of the core shell principal domain. In fact, we identified multiple inner surface-exposed residues of VP2 that, when simultaneously mutated, abolished the capacity of the core shell protein to activate VP1. The results of this study enhance our understanding of how rotavirus VP2 binds to and regulates the function of the viral polymerase.

MATERIALS AND METHODS

Generation of VP1- and VP2-expressing baculoviruses. The BaculoDirect expression system (Invitrogen) was used according to the manufacturer's protocol to create recombinant baculoviruses expressing the VP1 and VP2 proteins. Briefly, the VP1- and VP2-encoding genes were cloned into the entry vector pENTR-1A (see below) and then inserted into BaculoDirect C-Term linear DNA by recombination with LR clonase II. The baculovirus DNA was then transfected into *Spodoptera frugiperda* (Sf9) cells, and recombinant virus was harvested from the medium. Baculoviruses expressing VP1 and VP2 proteins of rotavirus strains SA11 and Bristol were generated as described previously (13).

The cDNAs for strain PO-13 VP1 (with a carboxy-terminal His tag), strain PO-13 VP2, and strain ETD VP2 were codon optimized and synthesized *de novo* by Geneart (Regensburg, Germany). These synthetic genes were then cloned into pENTR-1A using 5′ BamHI and 3′ NotI restriction sites. The amino acid sequences of PO-13 VP1, PO-13 VP2, and ETD VP2 exactly match sequences in the GenBank database (accession numbers AB009629, AB009630, and GQ479948, respectively).

To create pENTR-1A vectors for the generation of baculoviruses expressing SA11 VP2 with amino-terminal truncations (Δ10, Δ36, and Δ102), PCR was performed by using Platinum *Taq* (Invitrogen) as the enzyme and pENTR-SA11-VP2 as the template (13). The PCR products were cloned directly into pGEM-T Easy (Promega) and sequenced across the VP2-encoding region prior to subcloning into pENTR-1A using restriction sites (5′ EcoRI and 3′ NotI).

Blunt-end PCR was used to engineer pENTR-1A vectors for the generation of baculoviruses expressing chimeric VP2 proteins. For the subdomain chimeras (CHIMs) (CHIMs 1 to 4), the vector sequence was amplified by using outward PCR, nonphosphorylated primers, and pENTR-Bristol-VP2 as a template (13). The insert sequence was amplified by using 5′-phosphorylated primers and pENTR-SA11-VP2 as a template (13). For the multipoint (MP) mutants, a cDNA encoding Bristol VP2 in which nonconserved, inner surface-exposed residues were changed to those of SA11 VP2 (i.e., MP-VP2) was synthesized *de novo* by Geneart (Regensburg, Germany). The synthetic gene was cloned into pENTR-1A using 5′ BamHI and 3′ NotI restriction sites to create pENTR-MP-VP2. PCR was used to create pENTR-1A vectors encoding Bristol VP2 that contained the SA11 mutations only in the apical subdomain (pENTR-MP-api), the central subdomain (pENTR-MP-cent), or both the apical and central subdomains (pENTR-MP-both). Specifically, the vector sequence was amplified by using outward PCR, nonphosphorylated primers, and pENTR-Bristol-VP2 as a template. The insert sequence was amplified by using 5′-phosphorylated primers and pENTR-MP-VP2 as a template. In all reactions, Accuprime *Pfx* Supermix (Invitrogen) was used as the enzyme. The PCR products were treated with DpnI (New England BioLabs [NEB]) for 1 h at 37°C, and the cDNAs were gel purified prior to blunt-end ligation using T4 DNA ligase (NEB) for 1 h at 25°C. The final pENTR-1A vectors were sequenced across the entire VP2-encoding region to ensure the proper ligation of the insert and the absence of secondary mutations. Primer sequences used for cloning are available upon request.

Purification of recombinant VP1 and VP2. To prepare His-tagged SA11, PO-13, and Bristol VP1 proteins, 4×10^7 adherent Sf9 cells were infected at a multiplicity of infection (MOI) of approximately 5 with the appropriate baculovirus and maintained in TNH-FH medium (Invitrogen) containing 10% fetal bovine serum (FBS) for 4 days at 20°C. Infected cells were washed twice with cold phosphate-buffered saline (PBS), resuspended in 10 ml of cold VP1 lysis buffer (25 mM $NaHPO_4$, 200 mM NaCl [pH 7.8]), and sonicated. The insoluble fraction was removed by centrifugation at 15,000 × *g* for 10 min at 4°C, and His-tagged VP1 was recovered from the soluble fraction by incubation with cobalt resin (Talon) for 1.5 h at 4°C. The purified VP1 proteins bound to resin were washed using lysis buffer and then eluted using 300 μl lysis buffer containing 300 mM imidazole. Purified VP1 preparations were dialyzed against low-salt buffer (2 mM Tris-HCl [pH 7.5], 0.5 mM EDTA, 0.5 mM dithiothreitol) and stored at 4°C.

To prepare VP2 proteins, 2×10^8 spinner Sf9 cells were infected at an MOI of approximately 5 with the appropriate baculovirus and maintained in TNH-FH medium containing 10% FBS for 72 h at 28°C. Infected cells were washed twice with cold PBS and resuspended in 25 ml of cold low-salt buffer. Cells were lysed by the addition of deoxycholic acid to a 1% final concentration and by sonication. The VP2 proteins were pelleted through a 5-ml cushion of 35% (wt/vol) sucrose in low-salt buffer by centrifugation at 80,000 × *g* for 90 min at 12°C. Purified VP2 proteins were resuspended in 500 μl of low-salt buffer containing 1× complete protease inhibitor (Roche) and stored at 4°C.

The concentrations of the VP1 and VP2 proteins were determined by comparison with known amounts of standards electrophoresed in SDS-polyacrylamide gels and stained with PageBlue (Fermentas). The average purifications yielded approximately 2 to 10 μg of VP1 (per 4×10^7 cells) and 800 to 1,000 μg of VP2 (per 2×10^8 cells). Despite expressing equally well in Sf9 cells, the average yield of PO-13 VP1 following cobalt affinity purification was 3-fold less than that of SA11 or Bristol VP1.

Preparation of SA11 gene 8 RNA. To generate cDNA templates containing authentic 5′ and 3′ ends for T7 promoter-driven *in vitro* transcription, PCR was performed by using Accuprime *Pfx* Supermix (Invitrogen) and pSP65g8R as a template (13). The PCR-amplified cDNA was extracted twice with phenol-chloroform-isoamyl alcohol and once with chloroform and precipitated using isopropanol, prior to serving as a template for the T7 MEGAscript transcription system (Ambion) according to the manufacturer's instructions. The SA11 gene 8 products of transcription reactions were cleaned by using phenol-chloroform-isoamyl alcohol extraction and Quick Spin RNA minicolumns (Roche). The RNA quantity was determined by using a UV spectrophotometer (optical density at 260 nm [OD_{260}]), and RNA quality was assessed by electrophoresis in 7 M urea–5% polyacrylamide gels stained with ethidium bromide.

***In vitro* dsRNA synthesis assays.** Reaction mixtures contained 50 mM Tris-HCl (pH 7.1); 1.5% polyethylene glycol; 2 mM dithiothreitol; 1.5 units of RNasin (Promega); 20 mM magnesium acetate; 4 mM $MnCl_2$; 1.25 mM each ATP, CTP, UTP, and GTP; 10 μCi of [α-^{32}P]UTP (3,000 Ci/mmol); 8 pmol of SA11 gene 8 template; 1 to 2 pmol of VP1; and 10 to 20 pmol of VP2 (1:10 ratio of VP1 to VP2). Reactions proceeded at 37°C for 3 h, and the radiolabeled dsRNA was visualized following SDS-polyacrylamide gel electrophoresis and autoradiography. Figure images were generated by using Adobe Photoshop 9.0 and Adobe Illustrator 12.0.

Sequence and structural analyses. The VP1 and VP2 gene sequences of murine rotavirus strain EB were determined according to a method described previously by Rippinger et al. (22). Briefly, viral RNA was harvested from intestinal homogenates of EB-infected neonatal BALB/c mice (gift from H. Greenberg, Stanford University). The VP1- or VP2-encoding genes were amplified with the Superscript One-Step reverse transcription (RT)-PCR kit (Invitrogen) and sequenced by using the ABI Prism BigDye v3.1 terminator cycle sequencing kit and a 3730 DNA analyzer (Applied Biosystems).

Phylogenetic analyses and amino acid alignments were constructed by using MacVector 8.1.2. (Accelrys). Amino acid dendrograms were generated by using the neighbor-joining method (1,000 bootstrap repetitions) and the Poisson correction parameter. Amino acid alignments were constructed with MacVector 8.1.2 using ClustalW, BLOSUM series, with the defaults set (open-gap penalty of 10.0, extended-gap penalty of 0.05, and delay divergence of 40%). The GenBank accession numbers for all of the VP1 and VP2 sequences used in this study are listed in Table S1 in the supplemental material.

Structural analyses were performed by using the crystallographic data for the VP2 layer of bovine rotavirus strain UK (Protein Data Bank [PDB] accession number 3KZ4). Figure images were generated by using the UCSF Chimera molecular modeling system (21).

Nucleotide sequence accession numbers. The sequences deduced here were deposited into the GenBank database under accession numbers HQ540507 and HQ540508.

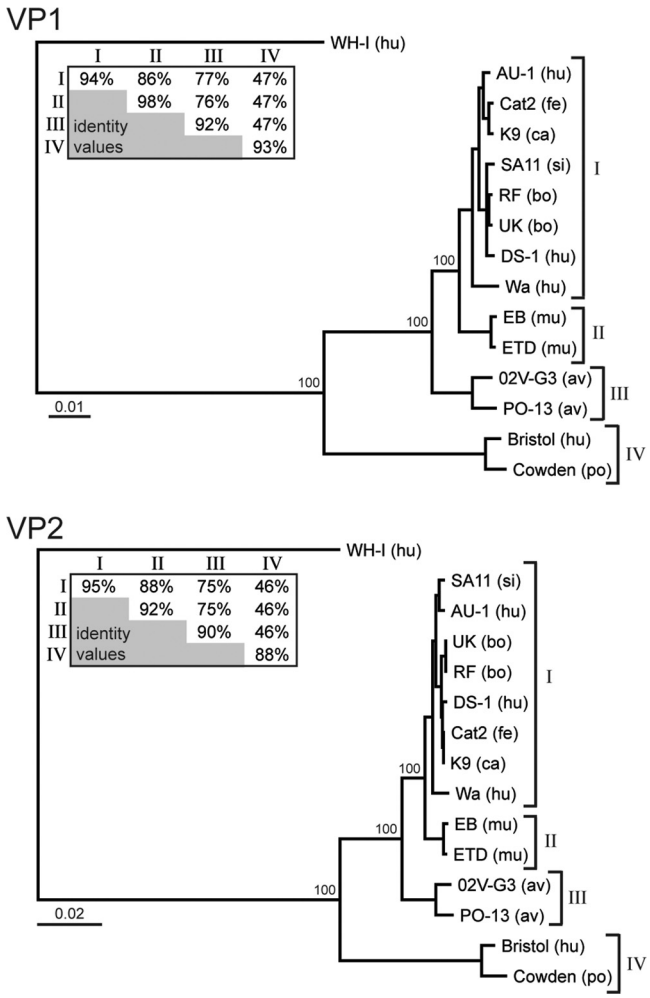

FIG. 2. Genetic divergence of VP1 and VP2 from different rotavirus strains. Phylogenetic dendrograms of VP1 (top) or VP2 (bottom) were constructed by using the amino acid sequences and the neighbor-joining method (1,000 bootstrap repetitions). The virus strain is listed with the species of isolation in parentheses: human (hu), simian (si), bovine (bo), porcine (po), feline (fe), canine (ca), murine (mu), and avian (av). The proteins of a group B rotavirus (strain WH-1) were used to root the trees. Bootstrap values are shown as percentages for key nodes. Brackets indicate the designated category (category I, II, III, or IV) of the VP1 and VP2 proteins. The average intra- and intercategory percent amino acid identities (identity values) are shown in the inset tables. The scale bar represents the number of substitutions per amino acid position.

RESULTS

Genetic limitations of VP1-VP2 compatibility. Nucleotide sequences of the VP1- and VP2-encoding segments have been determined for several human and animal rotaviruses. By creating phylogenetic dendrograms using the deduced amino acid sequences, we found that the polymerases and core shell proteins of each strain could be assigned into one of four distinct categories (categories I to IV) (Fig. 2). Category I is comprised of proteins from most group A rotaviruses, including those of the well-characterized laboratory animal strains (SA11, UK, and RF) and of prototype human strains (Wa and DS-1). Categories II and III are made up of proteins from group A murine and avian strains, respectively, while category IV is comprised of the VP1 or VP2 proteins of group C rotaviruses. VP1 or VP2 proteins belonging to the same category have a higher degree of sequence identity (88 to 98%) than do proteins belonging to different categories (46 to 88%). In fact, group C rotavirus category IV proteins are the most divergent, sharing only 46 to 47% sequence identity with group A rotavirus proteins of category I, II, or III (Fig. 2). Given the observed genetic variation, we sought to determine whether VP2 proteins belonging to different categories could functionally substitute for each other *in vitro*. Using baculovirus vectors, we expressed recombinant core shell proteins that represent each category: SA11 (category I), ETD (category II), PO-13 (category III), and Bristol (category IV). The VP2 proteins were purified from infected insect cells using ultracentrifugation and assayed for the capacity to support *in vitro* dsRNA synthesis by the VP1 protein of SA11 (category I), PO-13

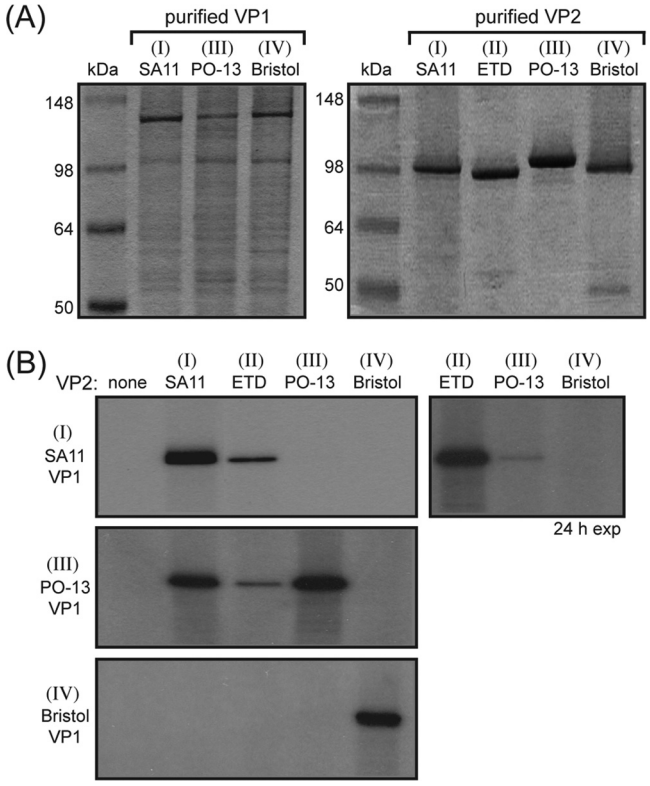

FIG. 3. Functional compatibility of VP1 and VP2 proteins. (A) Purified VP1 and VP2 proteins. Recombinant proteins were expressed in insect cells using baculovirus vectors and purified as described in Materials and Methods. The designated category (category I, II, III, or IV) of each protein is shown in parentheses above the strain. Samples containing approximately 2 pmol of VP1 or 20 pmol of VP2 were electrophoresed in a 10% SDS-polyacrylamide gel and visualized by PageBlue staining. Molecular mass markers are shown (in kilodaltons). (B) *In vitro* dsRNA synthesis by SA11 (top), PO-13 (middle), or Bristol (bottom) VP1. The designated category (category I, III, or IV) of each polymerase is shown in parentheses above the strain. Reactions proceeded in the absence (none) or presence of the different core shell proteins listed above the gels. Radiolabeled dsRNA products were resolved with 10% SDS-polyacrylamide gels and detected by autoradiography. The images on the left represent 4-h exposures (exp) of the gels to film. To visualize SA11 VP1 activity in the presence of PO-13 VP2, the gel was exposed to film for 24 h.

(category III), or Bristol (category IV) (Fig. 3A). Because it is replicated efficiently by both the SA11 and Bristol VP1 proteins, the SA11 gene 8 plus-strand RNA was used as a template in these experiments (13).

The results showed that the SA11 and ETD VP2 proteins supported SA11 VP1-mediated dsRNA synthesis but that Bristol VP2 did not (Fig. 3B). PO-13 VP2 induced SA11 VP1 to synthesize very minimal levels of dsRNA that were detected only following a long exposure of the gel to film (Fig. 3B). However, the PO-13 and Bristol VP2 proteins induced efficient dsRNA synthesis by their cognate polymerases (PO-13 VP1 and Bristol VP1, respectively), demonstrating that they are functional core shell proteins (Fig. 3B). Interestingly, the SA11 and ETD VP2 proteins also supported PO-13 VP1-mediated dsRNA synthesis albeit to various extents and less efficiently than that of PO-13 VP2 (Fig. 3B). The results also showed that Bristol VP2 was exquisitely specific for its own polymerase and did not support any detectable dsRNA synthesis by SA11 or PO-13 VP1, even after the overexposure of the gel to film (Fig. 3B and data not shown). Together, these results demonstrate that all rotavirus polymerases tested (SA11, PO-13, and Bristol VP1 proteins) exhibit VP2-dependent *in vitro* enzymatic functions and that each one is activated most efficiently by its cognate core shell protein. The phenotypic differences of the SA11, ETD, PO-13, and Bristol VP2 proteins seen in these experiments verify that the VP1-VP2 interaction(s) that leads to polymerase activation is specific.

Role of the VP2 5-fold hub in VP1 activation. To elucidate VP2 amino acids that correlate with polymerase activation specificity during *in vitro* dsRNA synthesis, we created an alignment using several core shell protein sequences (see Fig. S1 in the supplemental material). We observed that the VP2 principal domain (residues ~100 to 880) is more conserved among proteins in categories I to IV than is the VP2 amino terminus (residues ~1 to 100) (Fig. 4A and see Fig. S1 in the supplemental material). In fact, the region of VP2 that oligomerizes beneath each 5-fold axis to create an internal hub varies dramatically in both sequence and length among rotavirus strains; there is <10% amino acid identity between category I and IV amino termini. Given the observed variation and previous biochemical results, we hypothesized that the VP2 5-fold hub directly engages VP1 in a sequence-specific manner, thereby triggering the activity of the enzyme.

The architecture of the VP2 5-fold hub is not entirely known, but residues D18 to N31 of bovine strain UK (category I) create a single α-helix that clusters with those of neighboring monomers to form a vertical bundle seen in the X-ray crystal structure (Fig. 4B) (12). The extreme amino-terminal ~17 residues of VP2 are predicted to be located at the top of the bundle, near the inner shell wall, while the remaining residues (residues ~32 to 100) are thought to connect the hub to the principal domain (Fig. 4B) (12). To determine which putative 5-fold hub regions are involved in polymerase activation, we created baculoviruses that express SA11 VP2 with amino-terminal truncations (Fig. 4 and 5). The mutant core shell proteins were engineered to delete residues leading up to the vertical bundle (Δ10), up to and including the vertical bundle (Δ36), or the entire 5-fold hub (Δ102) (Fig. 4 and 5A). The truncated VP2 proteins were purified under the same conditions as those used for wild-type SA11 VP2 and were assayed for the capacity to support SA11 VP1-mediated *in vitro* dsRNA synthesis (Fig. 5B and C). Several lower-molecular-weight bands copurified with the truncation mutants; while the origin of these proteins is unclear, they might represent VP2 degradation products. Still, the results show that the deletion of the first 10 or 36 residues of SA11 VP2 dramatically reduced dsRNA synthesis, and the deletion of the entire 5-fold hub resulted in the abolishment of *in vitro* genome replication by VP1 (Fig. 5C). These data extend previous findings by Patton et al. regarding the importance of the VP2 amino terminus and suggest that all regions of the 5-fold hub are required for efficient polymerase activation (19).

To directly test the possibility that the VP2 5-fold hub activates VP1 in a specific manner, baculoviruses were engineered to express chimeric proteins in which the amino terminus (residues ~1 to 100) of SA11 VP2 was replaced with that of Bristol VP2 (Br:SA), and vice versa (SA:Br) (Fig. 6A and B). We

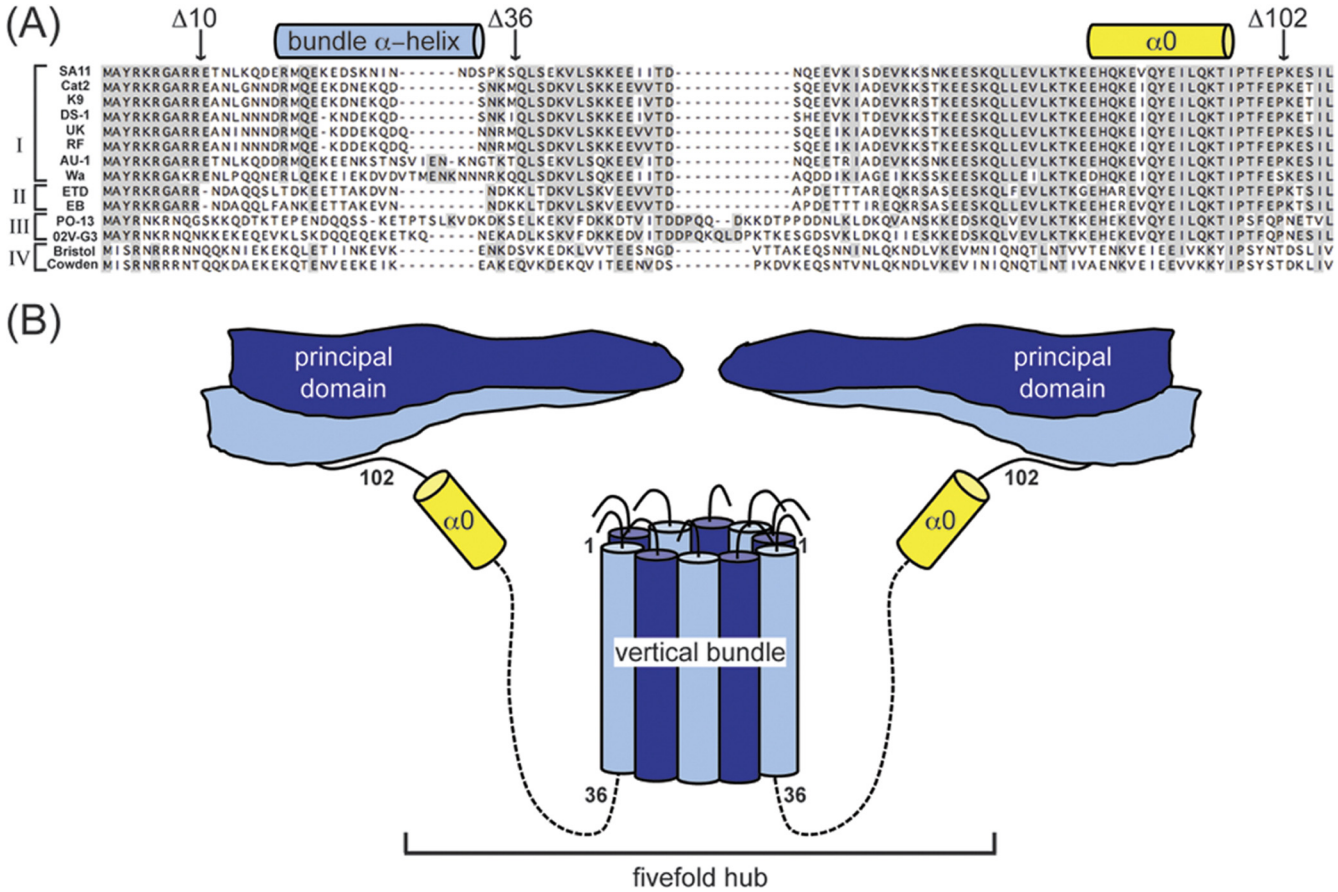

FIG. 4. Sequence and predicted architecture of the VP2 5-fold hub. (A) Alignment of the rotavirus VP2 amino termini. The VP2 amino acid sequences of several representative virus strains are shown. Dashes indicate gaps in the protein sequence, and shading reveals the conservation of amino acid identity. Brackets indicate the designated category (category I, II, III, or IV) of the VP2 proteins based on phylogenetics. The residues comprising the bundle α-helix (light blue cylinder) and the first visible helix in the crystal structure (α0) (yellow cylinder) are shown schematically, as are the sites of truncations for the experiments described in the legend of Fig. 5. (B) Cartoon rendering of the VP2 5-fold hub. Type A and B monomers are shown in dark blue and light blue, respectively. The VP2 amino termini (residues ~1 to 100) of 10 abutting monomers in a decamer unit oligomerize underneath the 5-fold axis. Residues 18 to 31 form an α-helix that clusters with those of neighboring monomers to create a 10-helix vertical bundle. Only the principal domains of two dimers and the hub connections of two monomers are shown for simplicity. The cartoon is meant to roughly illustrate the approximate shape and location of the 5-fold hub, the vertical bundle, α0 (yellow), and the principle domain (comprised of residues ~100 to 880) and is not drawn to scale.

expected that by swapping the 5-fold hubs of these VP2s, the enzyme specificity of the core shell proteins would switch. In contrast to what we anticipated, Br:SA supported SA11 VP1-mediated *in vitro* dsRNA synthesis, while SA:Br supported that of Bristol VP1 (Fig. 6C). These results indicate that the VP2 residues that correlate with polymerase activation specificity are actually located in the principal domain (residues ~100 to 880) rather than the amino terminus. Still, the levels of dsRNA in the presence of chimeric proteins were lower than those with the wild-type controls, supporting the notion that the hub plays an important role in genome replication.

VP2 subdomains critical for VP1 activation specificity. The principal domain of each VP2 monomer can be structurally delineated into three subdomains (apical, central, and dimer forming) (Fig. 7A) (12). In an effort to narrow down the locations of VP2 residues involved in VP1 activation specificity, baculoviruses were engineered to express chimeric proteins in which the subdomains of Bristol VP2 proteins were replaced with those of SA11 VP2. In particular, chimeras (CHIMs) 1, 2, and 3 have the SA11 VP2 apical, central, and dimer-forming subdomains, respectively, in a Bristol VP2 background (Fig. 7B). CHIM 4 contains both the SA11 VP2 apical and central subdomains (Fig. 7B). All of the chimeric proteins have the Bristol VP2 amino-terminal 5-fold hub residues (M1 to T105). These mutant Bristol VP2 proteins were expressed and purified in the same manner as that used for the wild-type controls and were assayed for a gain-of-function activation of noncognate SA11 VP1 *in vitro* (Fig. 7C and D).

We found that CHIMs 1 and 2 did not support *in vitro* dsRNA synthesis by either SA11 or Bristol VP1, suggesting that the residues essential for polymerase activation specificity may reside in more than one subdomain. CHIM 3 maintained its specificity for activating its cognate polymerase (i.e., Bristol VP1) and was incapable of supporting SA11 VP1-mediated dsRNA synthesis (Fig. 7D). This result indicates that the dimer-forming subdomain is not involved in polymerase activation specificity and suggests that the apical and/or central subdomain may be essential (Fig. 7D). In support of this conclu-

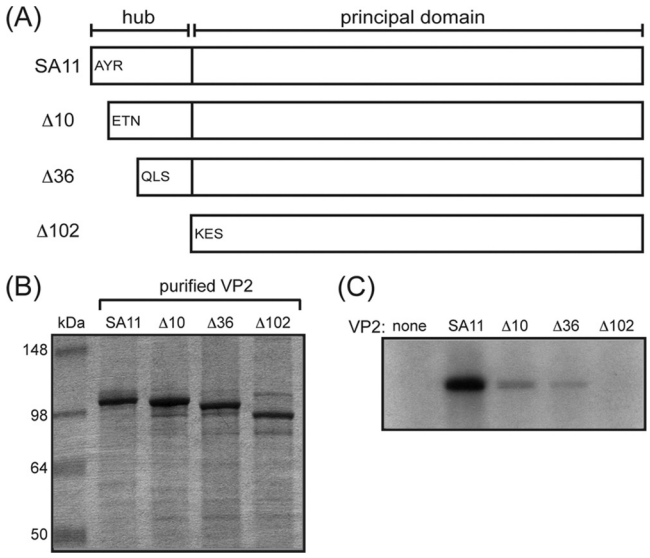

FIG. 5. Truncation mutagenesis of the SA11 VP2 5-fold hub. (A) Cartoon schematics of wild-type and mutant SA11 VP2 proteins. The residues contributing to the 5-fold hub are delineated from those of the principal domain by a black line. The three amino acids that follow the starting methionine are listed for the wild type (SA11) and each mutant protein (Δ10, Δ36, and Δ102). (B) Purified VP2 proteins. VP2 proteins were electrophoresed in a 10% SDS-polyacrylamide gel and visualized by PageBlue staining. Molecular size markers are shown (in kilodaltons). (C) *In vitro* dsRNA synthesis by SA11 VP1. Reactions proceeded in the absence (none) or the presence of the different core shell proteins listed above the gel. Radiolabeled dsRNA products were resolved with 10% SDS-polyacrylamide gels and detected by autoradiography.

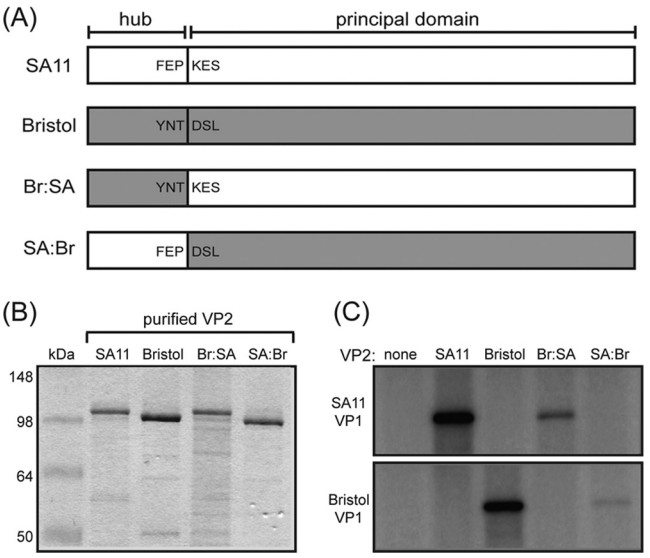

FIG. 6. Fivefold hub chimeric VP2 proteins. (A) Cartoon schematics of wild-type and chimeric VP2 proteins. Wild-type SA11 and Bristol VP2 proteins are shown in white and gray, respectively. The residues contributing to the 5-fold hub are delineated from those of the principal domain by a black line. Schematics of the 5-fold hub chimeras (Br:SA and SA:Br) are shown, with the parental origin of amino acids indicated by color (white for SA11 or gray for Bristol). The three amino acids before and after the fusion site are listed. (B) Purified VP2 proteins. VP2 proteins were electrophoresed in a 10% SDS-polyacrylamide gel and visualized by PageBlue staining. Molecular size markers are shown (kilodaltons). (C) *In vitro* dsRNA synthesis by SA11 or Bristol VP1. Reactions proceeded in the absence (none) or the presence of the different core shell proteins listed above the gels. Radiolabeled dsRNA products were resolved with 10% SDS-polyacrylamide gels and detected by autoradiography.

sion, SA11 VP1 showed robust activity in the presence of CHIM 4 (Fig. 7D). Essentially, by providing Bristol VP2 with the apical and central subdomains of SA11 VP2, this core shell protein gained the capacity to activate a noncognate polymerase. Despite having a Bristol VP2 amino terminus, the level of dsRNA made in the presence of CHIM 4 was nearly identical to that made with wild-type SA11 VP2 (Fig. 7D). This observation is interesting given that SA11 VP1 showed reduced dsRNA synthesis with Br:SA VP2 in previous experiments (Fig. 6C). It is possible that the precise sequence of the VP2 5-fold hub may not be as important as its context to the dimer-forming subdomain.

VP1 activation requires multiple VP2 apical and central subdomain residues. The apical and central subdomains of the VP2 shell are relatively conserved among category I to IV proteins, allowing for an unambiguous alignment of amino acid residues (Fig. 8 and see Fig. S1 in the supplemental material). However, in these regions, there are numerous amino acids that differ between the core shell proteins of SA11 and Bristol (Fig. 8). To determine which of these nonconserved residues could participate in sequence-specific VP1 binding and activation, we mapped their three-dimensional locations onto the high-resolution VP2 structure (Fig. 9A) (12). We identified 16 apical and 59 central nonconserved subdomain amino acids that are located on the inner surface of the core shell and have downward-pointing side chains (Fig. 8 and 9A). To test the importance of these core shell residues in VP1 activation, we engineered baculoviruses to express multipoint (MP) Bristol VP2 proteins in which the identified amino acids of the apical or central subdomain were simultaneously changed to the corresponding residues of SA11 VP2 (MP-api and MP-cent, respectively) (Fig. 9A and B). We also created a baculovirus that expresses Bristol VP2 with all 75 identified apical and central subdomains residues changed to match those of SA11 VP2 (MP-both) (Fig. 9A and B). Again, these mutant proteins were expressed and purified in the same manner as that used for the wild-type controls and were assayed for a gain-of-function activation of noncognate SA11 VP1 *in vitro* (Fig. 9B and C).

We found that the mutant Bristol VP2 proteins (MP-api, MP-cent, and MP-both) were all unable to support *in vitro* dsRNA synthesis by SA11 VP1 (Fig. 9C). This result demonstrates that that the introduced changes were not sufficient to switch the polymerase specificity of the core shell protein; additional residues within the apical and/or central subdomain must be involved (Fig. 8). Interestingly, we detected very low levels of dsRNA synthesis by Bristol VP1 in the presence of MP-api (Fig. 9C). This result suggests that the introduced apical subdomain mutations severely weakened, but did not abolish, cognate polymerase binding. In contrast, MP-cent and MP-both did not support any detectable Bristol VP1-mediated *in vitro* dsRNA synthesis, suggesting that the mutagenesis of the central subdomain prevented the polymerase interaction(s) (Fig. 9C). Together, these data indicate that multiple residues

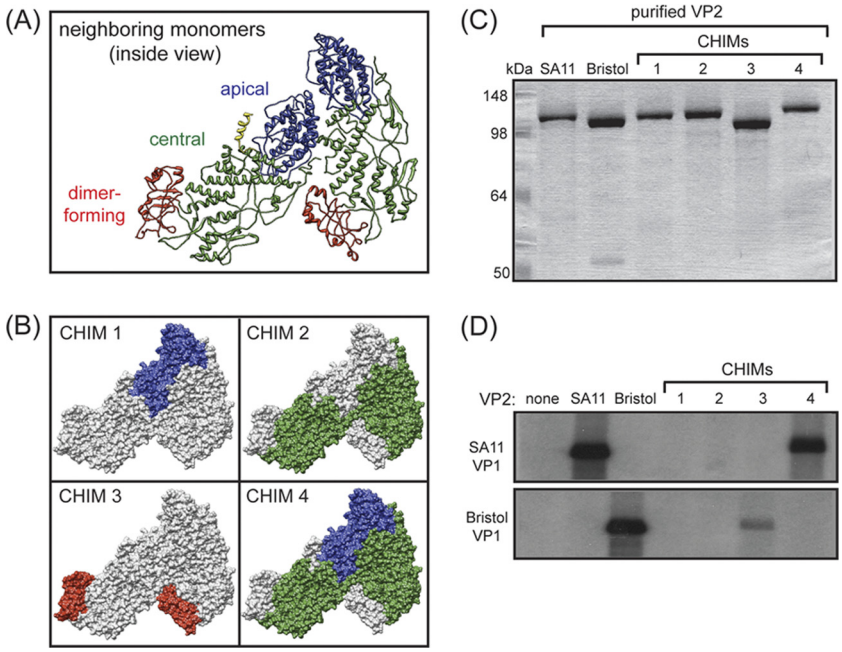

FIG. 7. Subdomain chimeric VP2 proteins. (A) Ribbon representation of neighboring VP2 monomers in a dimeric unit (inside view). The apical, central, and dimer-forming subdomains are in blue, green, and red, respectively. The resolved portion of the VP2 amino terminus in the type B monomer (residues 81 to 100) is in yellow. (B) Surface representations of chimeric (CHIM) VP2 proteins. In all images, gray indicates Bristol VP2 residues, while color indicates SA11 VP2 residues. (C) Purified VP2 proteins. VP2 proteins were electrophoresed in a 10% SDS-polyacrylamide gel and visualized by PageBlue staining. Molecular size markers are shown (in kilodaltons). (D) *In vitro* dsRNA synthesis by SA11 or Bristol VP1. Reactions proceeded in the absence (none) or the presence of the different core shell proteins listed above the gel. Radiolabeled dsRNA products were resolved with 10% SDS-polyacrylamide gels and detected by autoradiography.

of the VP2 apical and central subdomains are involved in VP1 activation.

DISCUSSION

The rotavirus RNA-dependent RNA polymerase performs all stages of RNA synthesis in association with an assembled or assembling VP2 core particle (15). Viral transcription occurs in the context of a DLP, whereby VP1 utilizes the minus strand of an associated dsRNA genome segment as a template for the creation of capped, nonpolyadenylated plus-strand RNAs (6, 15). In addition to serving as templates for protein synthesis, plus-strand RNAs are selectively packaged into forming VP2 core shells and act as templates for dsRNA synthesis. While the order of protein and RNA interactions that occur during packaging and genome replication is not completely understood, cumulative biochemical and structural data suggest a working model (4, 11, 18, 23, 24). First, individual copies of VP1 (with VP3) are thought to bind to the 3′ termini of the viral plus-strand RNAs, creating 11 different enzyme-RNA complexes (4, 11, 18, 24). The polymerase interacts with viral plus-strand RNA in a sequence-specific manner but positions the template out-of-register with the catalytic site (11). Thus, the VP1/VP3/plus-strand RNA complexes that first form in the viroplasm are thought to be catalytically inactive; the polymerases would have to undergo one or more conformational changes to synthesize dsRNA (11, 23). The autoinhibited RNA-binding mechanism of VP1 may allow time for assortment to occur so that one of each of the 11 VP1/VP3/plus-strand RNAs is incorporated into an assembling core. Interactions among VP1, VP2, and VP3 with each other and with the inclusion-forming nonstructural proteins (NSP2 and NSP5) are also likely to be important for regulating the timing of core assembly (1, 2). Following their assortment, VP2 would engage the polymerase component of VP1/VP3/plus-strand RNA complexes, thereby activating the enzymes to initiate minus-strand synthesis and produce dsRNA genome segments. Based on the observation that maximal *in vitro* dsRNA synthesis occurs with a 10:1 molar ratio of VP2 to VP1, we hypothesize that a decamer of VP2 activates each VP1 monomer (19, 24). Recombinant VP2 is heterogeneous in form, composed of assembly intermediates (dimers and decamers, etc.) and mixed multimers (bristly helix-like structures and sheet-like structures, etc.) in addition to T=1 core-like particles (7, 25). Therefore, whether a decamer is sufficient to activate a VP1 monomer remains to be experimentally confirmed. Nonetheless, the notion that a fully formed icosahedral core is not essential for polymerase activation is supported by the observation that the dsRNA products of *in vitro* genome replication are not encapsidated. In the process of dsRNA synthesis, however, the VP2 decamers must be brought together to form a complete, closed T=1 shell. In this model, the rotavirus core would be composed of 11 VP2 decamers with internally tethered VP1/VP3/plus-strand RNA complexes and a single empty vertex.

In the current study, we demonstrate that the VP2 core shell principal domain, rather than the amino terminus, correlates with polymerase activation specificity. This result was particularly surprising, as the VP2 amino terminus forms an internal

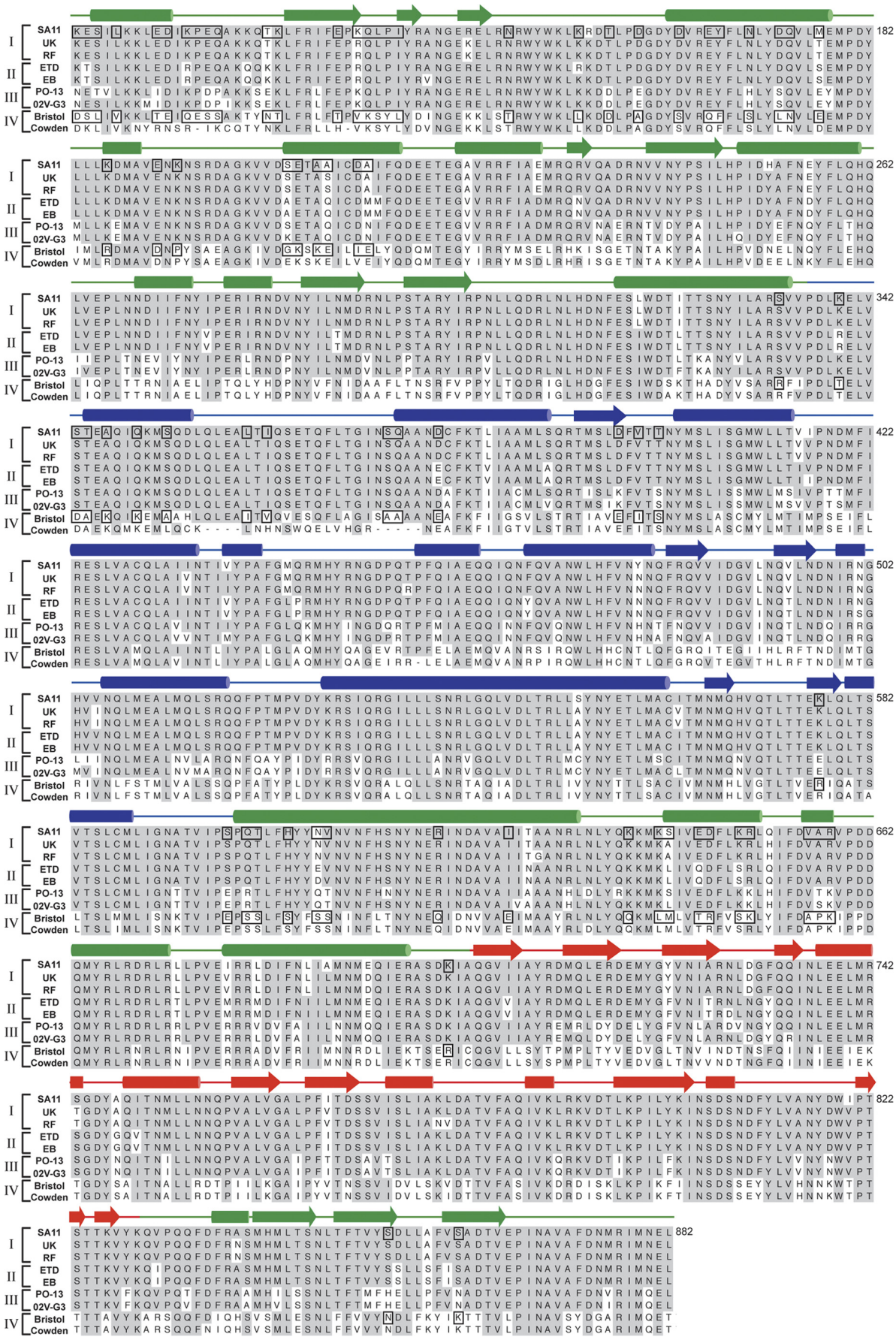

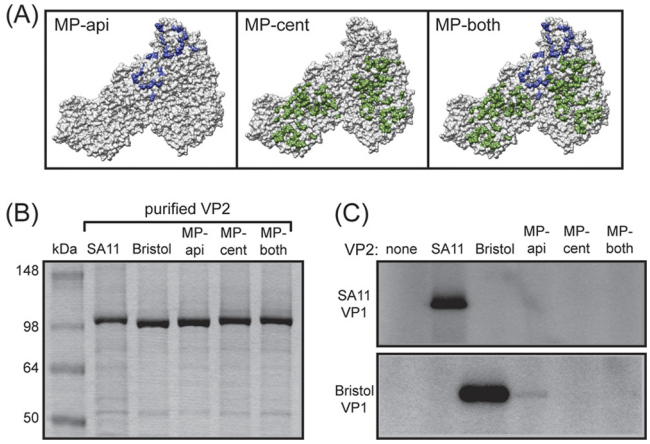

FIG. 9. Multipoint mutagenesis of Bristol VP2. (A) Three-dimensional location of amino acids identified in Fig. 8 (outlined residues) on the inner surface of the core shell. Neighboring VP2 monomers in a dimeric unit (inside view) are seen in a surface representation. Point mutations of residues of the apical (api) and central (cent) subdomains are shown in blue and green, respectively. Each Bristol VP2 residue at the colored sites was changed to match the corresponding residue of SA11 VP2. (B) Purified VP2 proteins. VP2 proteins were electrophoresed in a 10% SDS-polyacrylamide gel and visualized by PageBlue staining. Molecular size markers are shown (in kilodaltons). (C) *In vitro* dsRNA synthesis. Reactions proceeded in the absence (none) or the presence of the different core shell proteins listed above the gel. Radiolabeled dsRNA products were resolved with 10% SDS-polyacrylamide gels and detected by autoradiography.

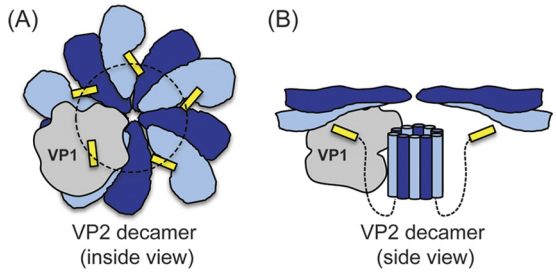

FIG. 10. Cartoon model of the VP1-VP2 interaction(s) that leads to polymerase activation. The images show cartoon renderings of a VP2 decamer interacting with a VP1 monomer. Type A and B monomers are in dark blue and light blue, respectively. Residues 1 to 81 of type B monomers are illustrated as yellow rectangles. VP1 (gray) is shown in relative scale binding to the VP2 core shell principal domain and juxtaposed to the 5-fold hub. (A) Inside view. The approximate scaled diameter of the hub is indicated as a black dotted line. (B) Side view as described in the legend of Fig. 4.

hub beneath each 5-fold axis and has long been known to be important for VP1 interactions. Specifically, previous studies have shown that this region of the core shell protein is dispensable for particle formation but is required for (i) the encapsidation of VP1 and VP3, (ii) interactions with RNA, and (iii) efficient *in vitro* dsRNA synthesis (8, 19, 26). Consistent with those results, we found that even a minor truncation of the VP2 amino terminus had dramatic effects on the capacity of the protein to support VP1-mediated dsRNA synthesis *in vitro* but did not prevent VP2/VP6 virus-like particle formation (data not shown). Moreover, chimeric VP2 proteins (SA:Br and Br:SA) that have their 5-fold hub residues replaced with those from a different strain supported lower levels of dsRNA synthesis by VP1. However, the reduced VP1 activation in the presence of the chimeric SA11 VP2 with a Bristol 5-fold hub (Br:SA) could be complemented by the addition of a Bristol dimer-forming subdomain (i.e., CHIM 4). This result was interesting, as the SA11 and Bristol VP2 amino termini are very divergent in sequence (<10% amino acid identity). It is possible that the 5-fold hub plays an indirect role in polymerase activation by helping to maintain the structural integrity of the principal domain via interactions with the dimer-forming subdomain. Deletion mutagenesis of the 5-fold hub or the substitution of a noncognate hub (without a matching dimer-forming subdomain) might have caused subtle defects in the presentation of the VP1-binding residues located in the apical and central subdomains. In support of this idea, cryo-electron microscopy studies of virus-like particles with amino-terminally truncated VP2 (bovine strain RF) revealed alterations in the vicinity of the 5-fold axis compared with the wild-type controls (9). We are now generating reagents for the production of Bristol VP2/VP6 virus-like particles to determine whether the chimeras exhibit structural defects.

Aside from maintaining the integrity of the principal domain, the 5-fold hub might also play important roles in other stages of viral replication. For example, during core shell assembly, interactions of VP2 amino termini may serve to enhance the kinetics of decamer formation. Additionally, the hub could be required for the initial engagement of the VP1/VP3/plus-strand RNA complex, bringing the polymerase in proximity to the activation residues in the VP2 apical and central subdomains. Such a "two-step" manner of core shell-polymerase interactions would confer another level of temporal control to rotavirus packaging and genome replication. Ongoing experiments are aimed at determining whether VP2 amino-terminal residues are involved directly in core formation efficiency and/or VP1 encapsidation. However, it is important that the VP2 5-fold hub is composed of 10 abutting amino termini of 100 amino acids in length and has a molecular mass of nearly 100 kDa (12). The diameter of the hub extends out to the first resolved helix (α0) of the type B VP2 monomers (Fig. 10) (12). At this size, the 5-fold hub would presumably block access to the apical subdomains of the VP2 monomers, which are important for VP1 activation *in vitro*. The internal 5-fold hub density attributed to VP2 amino termini has been detected only in the context of double-layered particles that have al-

FIG. 8. Alignment of the VP2 principal domain. The VP2 amino acid sequences of several representative virus strains are shown. Dashes indicate gaps in the protein alignment, and shading reveals the conservation of amino acid identity. Brackets indicate the designated category (category I, II, III, or IV) of the VP2 proteins based on the phylogenetic analyses described in the legend of Fig. 2. Subdomains are colored as described in the legend of Fig. 7, and secondary structural elements are shown above the corresponding residues (12). Amino acids outlined in black were targeted for multipoint (MP) mutagenesis in Fig. 9.

ready undergone genome replication (12). It is interesting to speculate that the amino terminus of VP2 does not form an organized hub-like structure until after enzyme activation and dsRNA synthesis. Alternatively, the fact that the 5-fold hub has been difficult to visualize in structural studies suggests that it is flexible and therefore might be capable of "bending" to accommodate VP1. It was also proposed previously that the VP2 5-fold hub serves as a conduit for the exit of plus-strand RNAs out of the core during transcription (12). The dramatic sequence variation and high concentration of charged amino acids in the VP2 amino terminus are consistent with this idea.

To date, every rotavirus polymerase that we have tested exhibits *in vitro* enzymatic activity that is dependent upon the presence of a core shell protein (13). While the group A rotavirus VP2 proteins (categories I to III) could substitute for each other to various degrees in our experiments, the group C Bristol VP2 (category IV) was completely incapable of functioning in place of any group A VP2. The lack of obvious gene reassortment between group A and C rotavirus strains might be a reflection of such incompatible viral proteins. Furthermore, analysis of protein sequences from different strains revealed that the VP1 and VP2 trees have nearly identical topologies and phylogenetic groupings. This result indicates that the polymerase and core shell proteins have coevolved and function best when kept together. Indeed, the observation that the SA11, PO-13, and Bristol polymerases are most active in the presence of VP2 from the same strain suggests that the protein-protein interaction(s) leading to enzyme activation is fairly specific. Thus, amino acids that differ among the SA11, ETD, PO-13, and Bristol VP2 proteins must be involved in creating the binding site(s) for VP1. In an attempt to identify such residues, we created Bristol VP2 proteins in which nonconserved, inner surface residues of the apical and/or central subdomains were changed to the corresponding residue of SA11 VP2 (MP-api, MP-cent, and MP-both). Our goal was to create Bristol VP2 proteins that gained the capacity to activate SA11 VP1. Unfortunately, the mutant proteins that we generated did not support SA11-mediated dsRNA synthesis *in vitro*, demonstrating that many more residues are involved. The Bristol VP2 mutants did, however, show reduced or no activation of cognate Bristol VP1 *in vitro*, suggesting that the identified residues are involved in this process. We cannot exclude the possibility that the introduced mutations caused gross structural defects in VP2. Due to the heterogeneous form of recombinant VP2, we are unable identify perturbations simply by visualizing the preparations using electron microscopy (7, 25). Moreover, the biochemical insolubility of recombinant VP2 precludes classical protein-protein interaction assays (gel filtration, sucrose gradient analyses, and pulldowns, etc.) to elucidate the multimerization status or VP1-binding capacities of the mutants (7, 25). However, because the targeted amino acids are all located on the core shell interior and have downward-pointing side chains, we think that it is likely that the mutations did directly affect the polymerase interaction(s). Given the size of VP1 (~125 kDa; ~70 Å in diameter), it is possible that its binding footprint (~1,400 Å^2) spans several monomers of a VP2 decamer (Fig. 10). The quasi-equivalent positioning of type A and B VP2 monomers also implies that both the apical and central subdomains are involved in VP1 binding and activation. Nevertheless, future studies are needed to more precisely identify the core shell amino acids critical for multifaceted interactions with the rotavirus polymerase.

ACKNOWLEDGMENTS

We thank Christine Rippinger for determining the VP1 and VP2 sequences of murine rotavirus strain EB and Daniel Luque for creating the VP2 core shell image reconstruction shown in Fig. 1. We also express our gratitude to Michelle Arnold, Kristen Ogden, Aitor Navarro, and Shane Trask for important scientific and editorial comments.

This study was supported by the Intramural Research Program of the National Institute of Allergy and Infectious Diseases, National Institutes of Health.

REFERENCES

1. **Arnoldi, F., M. Campagna, C. Eichwald, U. Desselberger, and O. R. Burrone.** 2007. Interaction of rotavirus polymerase VP1 with nonstructural protein NSP5 is stronger that that with NSP2. J. Virol. **81:**2128–2137.
2. **Berois, M., C. Sapin, I. Erk, D. Poncet, and J. Cohen.** 2003. Rotavirus nonstructural protein NSP5 interacts with major core protein VP2. J. Virol. **77:**1757–1763.
3. **Estes, M. K., and A. Z. Kapikian.** 2007. Rotaviruses and their replication, p. 1917–1974. *In* D. M. Knipe et al. (ed.), Fields virology, 5th ed. Lippincott Williams & Wilkins, Philadelphia, PA.
4. **Gallegos, C. O., and J. T. Patton.** 1989. Characterization of rotavirus replication intermediates: a model for the assembly of single-shelled particles. Virology **172:**616–627.
5. **Guglielmi, K. M., S. M. McDonald, and J. T. Patton.** 2010. Mechanism of intra-particle synthesis of the rotavirus double-stranded RNA genome. J. Biol. Chem. **285:**18123–18128.
6. **Jayaram, H., M. K. Estes, and B. V. Prasad.** 2004. Emerging themes in rotavirus cell entry, genome organization, transcription and replication. Virus Res. **101:**67–81.
7. **Labbe, M., A. Charpilienne, S. E. Crawford, M. K. Estes, and J. Cohen.** 1991. Expression of rotavirus VP2 produces empty corelike particles. J. Virol. **65:**2946–2952.
8. **Labbe, M., P. Baudoux, A. Charpilienne, D. Poncet, and J. Cohen.** 1994. Identification of the nucleic acid binding domain of the rotavirus VP2 protein. J. Gen. Virol. **75:**3423–3430.
9. **Lawton, J. A., et al.** 1997. Three-dimensional structural analysis of recombinant rotavirus-like particles with intact and amino-terminal-deleted VP2: implications for the architecture of the VP2 capsid layer. J. Virol. **71:**7353–7360.
10. **Li, Z., M. L. Baker, W. Jiang, M. K. Estes, and B. V. Prasad.** 2009. Rotavirus architecture at subnanometer resolution. J. Virol. **83:**1754–1766.
11. **Lu, X., et al.** 2008. Mechanism for coordinated RNA packaging and genome replication by rotavirus polymerase VP1. Structure **16:**1678–1688.
12. **McClain, B., E. Settembre, B. R. Temple, A. R. Bellamy, and S. C. Harrison.** 2010. X-ray crystal structure of the rotavirus inner capsid particle at 3.8 Å resolution. J. Mol. Biol. **397:**587–599.
13. **McDonald, S. M., D. Aguayo, F. D. Gonzalez-Nilo, and J. T. Patton.** 2009. Shared and group-specific features of the rotavirus RNA polymerase reveal potential determinants of gene reassortment restriction. J. Virol. **83:**6135–6148.
14. **McDonald, S. M., Y. J. Tao, and J. T. Patton.** 2009. The ins and outs of four-tunneled *Reoviridae* RNA-dependent RNA polymerases. Curr. Opin. Struct. Biol. **19:**775–782.
15. **McDonald, S. M., and J. T. Patton.** 2009. Core-associated genome replication mechanisms of dsRNA viruses, p. 201–224. *In* C. Cameron, M. Gotte, and K. D. Raney (ed.), Viral genome replication. Springer Science and Business Media, New York, NY.
16. **Mertens, P.** 2004. The dsRNA viruses. Virus Res. **101:**3–13.
17. **Patton, J. T.** 1996. Rotavirus VP1 alone specifically binds to the 3′ end of viral mRNA, but the interaction is not sufficient to initiate minus-strand synthesis. J. Virol. **70:**7940–7947.
18. **Patton, J. T., and C. O. Gallegos.** 1990. Rotavirus RNA replication: single-stranded RNA extends from the replicase particle. J. Gen. Virol. **71:**1087–1094.
19. **Patton, J. T., M. T. Jones, A. N. Kalbach, Y. W. He, and J. Xiaobo.** 1997. Rotavirus RNA polymerase requires the core shell protein to synthesize the double-stranded RNA genome. J. Virol. **71:**9618–9626.
20. **Pesavento, J. B., S. E. Crawford, M. K. Estes, and B. V. Prasad.** 2006. Rotavirus proteins: structure and assembly. Curr. Top. Microbiol. Immunol. **309:**189–219.
21. **Petterson, E. F., et al.** 2004. UCSF Chimera—a visualization system for exploratory research and analysis. J. Comp. Chem. **25:**1605–1612.
22. **Rippinger, C. M., J. T. Patton, and S. M. McDonald.** Complete genome sequence analysis of candidate human rotavirus vaccine strains RV3 and 116E. Virology **405:**201–213.
23. **Tao, Y., D. L. Farsetta, M. L. Nibert, and S. C. Harrison.** 2002. RNA synthesis in a cage—structural studies of reovirus polymerase λ3. Cell **111:**733–745.

24. **Tortorici, M. A., T. J. Broering, M. L. Nibert, and J. T. Patton.** 2003. Template recognition and formation of initiation complexes by the replicase of a segmented double-stranded RNA virus. J. Biol. Chem. **278:**32673–32682.
25. **Zeng, C. Q., et al.** 1994. Characterization of rotavirus VP2 particles. Virology **201:**55–65.
26. **Zeng, C. Q., M. K. Estes, A. Charpilienne, and J. Cohen.** 1998. The N terminus of rotavirus VP2 is necessary for encapsidation of VP1 and VP3. J. Virol. **72:**201–208.
27. **Zhang, X., et al.** 2008. Near-atomic resolution using electron cryomicroscopy and single-particle reconstruction. Proc. Natl. Acad. Sci. U. S. A. **105:**1867–1872.